

Could It Be Generated? Towards Practical Analysis of Memorization in Text-To-Image Diffusion Models

Zhe Ma
Zhejiang University
Hangzhou, China
mz.rs@zju.edu.cn

Xuhong Zhang
Zhejiang University
Hangzhou, China
zhangxuhong@zju.edu.cn

Qingming Li
Zhejiang University
Hangzhou, China
liqm@zju.edu.cn

Tianyu Du
Zhejiang University
Hangzhou, China
zjradty@zju.edu.cn

Wenzhi Chen
Zhejiang University
Hangzhou, China
chenwz@zju.edu.cn

Zonghui Wang
Zhejiang University
Hangzhou, China
zhwang@zju.edu.cn

Shouling Ji
Zhejiang University
Hangzhou, China
sji@zju.edu.cn

ABSTRACT

The past few years have witnessed substantial advancement in text-guided image generation powered by diffusion models. However, it was shown that text-to-image diffusion models are vulnerable to training image memorization, raising concerns on copyright infringement and privacy invasion. In this work, we perform practical analysis of memorization in text-to-image diffusion models. Targeting a set of images to protect, we conduct quantitative analysis on them without need to collect any prompts. Specifically, we first formally define the memorization of image and identify three necessary conditions of memorization, respectively similarity, existence and probability. We then reveal the correlation between the model’s prediction error and image replication. Based on the correlation, we propose to utilize inversion techniques to verify the safety of target images against memorization and measure the extent to which they are memorized. Model developers can utilize our analysis method to discover memorized images or reliably claim safety against memorization. Extensive experiments on the Stable Diffusion, a popular open-source text-to-image diffusion model, demonstrate the effectiveness of our analysis method.

1 INTRODUCTION

Diffusion probabilistic models [14, 39] have shown impressive capability in the generation of images [31, 32], videos [7], 3D point cloud [24], etc. These techniques lay the foundation for commercial systems or communities such as Stable Diffusion [32], Midjourney [4], DALL-E 2/3 [3, 31] and Imagen [33], which have attracted millions of active users. The popularity of diffusion models can be attributed to the hierarchical denoising procedure, which offers high stability when trained on billions of data [36] and scalability to multimodal conditional generation.

The large-scale dataset used to train the state-of-the-art text-to-image generation models, e.g., the open-source image-caption dataset LAION-5B [36], are widely acknowledged to contain content that will raise concerns about copyright and privacy. For example, as reported, LAION-5B could refer to photographers’ work without

authorization [12] and private medical photographs were also found therein [1]. With the uncurated data for training, diffusion models are likely to generate content that infringes the copyright of creators or exposes private information.

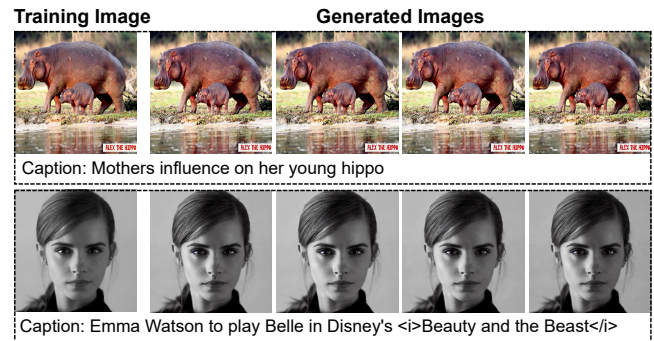


Figure 1: Examples of memorized images in Stable Diffusion. The right four random samples are all the same as the corresponding training image in the first column.

In this work, we focus on the problem of memorization in text-to-image diffusion models, a worst case of training data misuse. Memorization in text-to-image diffusion models is a failure of generation that, when input with certain prompt but different random seeds, a model always rigidly generates the same data as those in its training set. This type of generation is regarded as failed because a probabilistic generative model is supposed to generate novel and diversified images. Figure 1 illustrates two examples of memorization in Stable Diffusion. Memorization in text-to-image diffusion models is not only a technical problem analogous to mode collapse as Generative Adversarial Networks (GAN) [6], but also a prejudice to the interests of image owners. In terms of copyright protection, even the model developers are authorized to train their model with copyrighted images, the image owners will never expect their images to be replicated to arbitrary users as this would cause

indisciplinable dissemination. In past years, text-to-image models have been facing lawsuits for generating derivative images that mimic the style of artists. However, compared to derivative generations whose legality is still in pending [35], exact replication of copyrighted images is undisputedly intolerable. For privacy preservation, a series of works [16, 27] have proposed to use synthetic data in place of real data to prevent sharing of private information. For this goal, potential memorization should also be carefully circumvented. The existence of memorization in text-to-image models was first demonstrated by Carlini et al. [8] and Somepalli et al. [40, 41]. They studied the most popular open-source text-to-image diffusion model Stable Diffusion [32] and discovered prompts that trigger the model to generate training images.

Although text-to-image diffusion models are found to be vulnerable to memorization, a practical analysis method is still a challenging problem. First of all, existing analysis methods [8, 40, 41, 46] are all prompt-based: They first generate massive candidate images using captions from the original training set and then detect risky generations of low diversity [8], search for generated images highly similar to training images [40, 41] or detect prompts with high prediction errors [46]. The prompt-based analysis methods are unable to determine whether an arbitrary image is memorized or not. Actually they are unaware of which images might be memorized only after memorization has been discovered. Besides, for the other images whose training captions seem not trigger memorization phenomena, their safety against memorization is still uncertain and hard to be analyzed by existing methods, because it is impossible to exhaustively test all prompts. To this end, a practical analysis method is expected to be image-based rather than prompt-based. Second, a practical analysis method requires quantitative measurement of memorization. Previous works focus on the discovery of memorized images and lack accurate description of memorization for each instance. Quantitative measurement of memorization not only provides strong evidence for the security risks of memorized images, but allows model developers to responsibly claim safety for normal images to their owners.

To cope with the challenges, we consider a practical scenario where the model developers predefine a target set of copyrighted or privacy-preserving images. They aim to perform a security analysis on the target images to decide whether they are memorized by the model and to quantify the extent to which they are memorized. Based on the analysis, developers are able to claim the safety against memorization for the target images to their data providers, or discover memorized images in advance and fix the vulnerability.

To perform the security analysis, we first formally define image memorization in diffusion models and identify three conditions to say an image is memorized, named *similarity*, *existence* and *probability*. The *similarity* condition means that generated images should be exactly alike a target image. As mentioned before, this condition reflects the worst case misuse of training data and poses a significant security threat. Instead of calculating the similarity between generated images and target images, we utilize the model’s prediction error as a metric to recognize image replications. This metric is as effective as previous metrics in recognition of image replication. It also enables us to invert the model to find inputs that cause replication, based on which we conduct analysis for the other two conditions. The *existence* condition requires that there exist a

prompt to trigger the replication of a target image. We propose a prompt inversion algorithm to analyze this condition and verify by contradiction the existence of such prompt. The *probability* condition is fulfilled when a target image are frequently replicated at sampling time. We propose to measure the condition by comparing model’s prediction error on the target image to those of a safe model. If the target image would be replicated with high probability, a significant distribution shift away from the error distribution of the safe model can be observed. We verify by contradiction that the unconditional diffusion models trained on large-scale data are safe from memorization and thus utilized as the safe model. We conduct comprehensive experiments on Stable Diffusion to demonstrate the effectiveness of our analysis method.

In summary, we make the following contributions in this paper:

- We perform a more practical analysis on the memorization in text-to-image diffusion models. Our analysis method is image-based and does not need to collect massive prompts, which is more reliable than prompt-based analysis methods.
- We provide a formal definition of memorization in text-to-image diffusion models and identify three conditions of it. We then propose effective metrics and algorithms to measure each condition and ultimately quantify the extent to which the target images are memorized.
- We demonstrate the viability of our analysis method through detailed experiments on Stable Diffusion, which reveals the intrinsic properties of memorization in text-to-image diffusion models.

2 BACKGROUND

2.1 Diffusion Model

Diffusion probabilistic models [14, 39] are a class of latent variable models consisting of a hierarchy of denoising autoencoders. The encoder is not learned but replaced by a manually designed diffusion process. Given input image x_0 ¹ and a total of T steps, the diffusion process is modeled as a Markov chain that gradually adds Gaussian noises $\epsilon_{0:T-1}$ to the input image x_0 according to a weight schedule $\alpha_{1:T}$:

$$\begin{aligned} q(x_{1:T}|x_0) &= \prod_{t=1}^T q(x_t|x_{t-1}), \\ q(x_t|x_{t-1}) &= \mathcal{N}(x_t; \sqrt{\alpha_t}x_{t-1}, (1 - \alpha_t)\epsilon_{t-1}), \\ q(x_t|x_0) &= \mathcal{N}(x_t; \sqrt{\bar{\alpha}_t}x_0, (1 - \bar{\alpha}_t)\epsilon_0), \bar{\alpha}_t = \prod_{i=1}^t \alpha_i. \end{aligned} \quad (1)$$

$\bar{\alpha}_t$ gradually decreases to almost zero in the last step T so that x_T is close to pure Gaussian noise. The process of generating image x_0 is the reverse of the diffusion process and also a Markov chain starting at $x_T \sim \mathcal{N}(0, I)$:

$$p(x_{0:T}) = p(x_T) \prod_{t=1}^T p_\theta(x_{t-1}|x_t). \quad (2)$$

¹In this paper we intentionally confuse the use of x and x_0 to denote an image. In the contexts related to the diffusion process we use x_0 and otherwise x .

If the diffusion process is divided into sufficient steps, each reverse step $p_\theta(x_{t-1}|x_t)$ can be approximated by a Gaussian transformation that is trained to match the corresponding diffusion step $q(x_{t-1}|x_t, x_0)$. This is implemented by minimizing the following objective:

$$\mathcal{L} = \mathbb{E}_{t, x_0, \epsilon_0} [\|\epsilon_0 - \epsilon_\theta(x_t, t)\|_2^2], \quad (3)$$

where ϵ_θ is a neural network that predicts the added noise ϵ_0 , $x_t = \sqrt{\bar{\alpha}_t}x_0 + \sqrt{1 - \bar{\alpha}_t}\epsilon$. After training, the vanilla sampling procedure starts with a random Gaussian noise $x_T \sim \mathcal{N}(0, I)$ and removes the predicted noise stepwise by $x_{t-1} = \frac{1}{\sqrt{\alpha_t}}(x_t - \frac{1-\alpha_t}{\sqrt{1-\alpha_t}}\epsilon_\theta(x_t, t)) + \sigma_t\mathcal{N}(0, I)$, where $\sigma_t = \frac{\sqrt{(1-\alpha_t)(1-\bar{\alpha}_{t-1})}}{\sqrt{1-\alpha_t}}$ when $t > 1$ and 0 when $t = 1$. The vanilla sampling algorithm is extremely slow to generate an image as it must invoke the network ϵ_θ for T times (e.g., 1000 steps in Stable Diffusion). To mitigate the problem, a variety of efficient sampling algorithms are proposed, such as DDIM sampler [42], PLMS sampler [22], etc.

2.2 Conditional Diffusion Model

Diffusion models can be extended to conditional variants to generate images under the guidance of some input condition, e.g., object class, textual prompt. Text-to-image models are conditional diffusion models that allow users to input some prompts to indicate the desired content of generated images. There are mainly two types of guidance, i.e., Classifier Guidance [9] and Classifier-Free Guidance [15]. Classifier Guidance additionally trains a classifier on the noisy image x_t to predict its coupled condition c and utilizes the gradients from the classifier to guide the sampling. Most diffusion models like Stable Diffusion choose Classifier-Free Guidance because it does not need to train an extra classifier. Classifier-Free Guidance implicitly trains two models, an unconditional model $\epsilon_\theta(x_t, t)$ and a conditional model $\epsilon_\theta(x_t, t, c)$. The two models share parameters and the unconditional model is trained by randomly replacing input condition c with null (for textual condition, the unconditional model is always input an empty string). At sampling time, the predicted noise is a linear combination of unconditional prediction and conditional prediction:

$$\hat{\epsilon}_\theta(x_t, t, c) = \epsilon_\theta(x_t, t) + \gamma(\epsilon_\theta(x_t, t, c) - \epsilon_\theta(x_t, t)), \quad (4)$$

where a larger hyperparameter γ results in generated images more consistent with the input condition.

2.3 Text-To-Image Diffusion Model

An instance of conditional diffusion models, which we will study in this work, is text-to-image diffusion models. To obtain semantically meaningful condition c , the input prompt is first tokenized and projected into a sequence of continuous token embeddings $e = [e_0, e_1, \dots, e_{N-1}]$, where N is the number of tokens. The token embeddings are further encoded as the condition c by a pre-trained image-text model, for example, CLIP [29] or language model, for example, T5 [30]. Depending on the specific modeling, the condition c is either incorporated into the middle layers of the noise prediction network $\epsilon_\theta(x_t, t, c)$ via cross-attention [32, 33], or concatenated with a sequence of image tokens, modeling $\epsilon_\theta(x_t, t, c)$ autoregressively as a single stream [31].

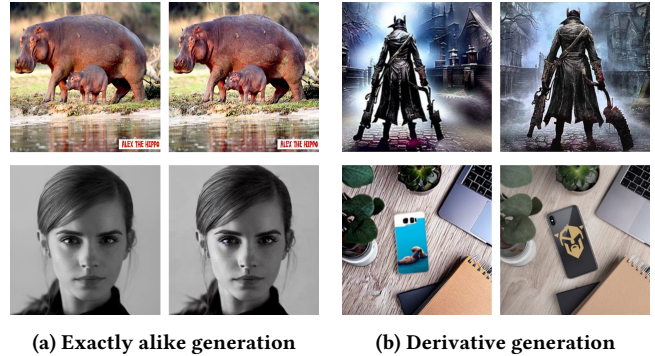


Figure 2: Examples of exactly alike generation and derivative generation.

Among the advanced text-to-image diffusion models, Stable Diffusion is open-sourced both in implementation and its training data, therefore we will utilize it for our study. To generate high-resolution images, Stable Diffusion first train an autoencoder which encodes an image x into a lower-dimensional representation $z = \mathcal{E}(x)$ perceptually equivalent to the data space. The diffusion model is trained in the reduced space. At sampling time, after generating a latent z' , a high-resolution image x' is obtained via the pre-trained decoder $x' = \mathcal{D}(z')$.

3 DEFINITION OF MEMORIZATION

We first formalize the definition of memorization and then make comparisons to existing ones:

Definition. A training sample x is memorized if, at sampling time, there exists a prompt, under whose guidance the model will generate samples that are exactly alike x with a significant probability. Exactly alike does not mean verbatim same or byte-by-byte match in the file system. It is still on the perception level but excludes even a minor transformation such as change in view point and component recombination.

Exactly alike training sample x , existence of a prompt and significant probability are three conditions to say a training sample is memorized. For brevity, we call them the *similarity*, *existence* and *probability* conditions. Existing works cover the three conditions to varying degrees.

Carlini et al. [8] provide a strict definition of memorization that a training image is eidetic memorized if it has at most k instances in the training set and is extractable from the model via some prompts. We both count it as memorization if the generated samples are exactly alike or eidetic to training ones (Figure 2a). Other works [40, 41, 46, 48] do not give a formal definition and discuss a wider scope of memorization in the form of derivative generation, such as partial copy and style-like copy (Figure 2b). Restricting memorization to the most extreme case "exactly alike" has several advantages over a wider scope. First, lawsuits against derivative actions in image generation models are still in very early stages [35]. It takes time to render decisions on its legality. In contrast, "exactly alike" memorization is by no means allowed if the related images are copyrighted or private. Second, from a technical perspective, diffusion models are inherently trained to replicate training samples

pixel by pixel, as in Equation 4. Therefore, "exactly alike" memorization is not only defined at the problem level, but also possible to find evidence in the model itself. This allows us to utilize the internal statistics of the model to measure its memorization problem, rather than relying on external models to match training images and generate images, which is less reliable due to potential risks such as adversarial attack [49].

The *existence* condition is not a concern for previous works as they analyze memorization in a prompt-based way such that the condition is always satisfied. For our image-based analysis, the condition is important to be able to expose realistic risks, as discussed later.

As for the *probability* condition, Carlini et al. do not involve the *probability* condition explicitly in the definition but in their membership inference attack designed to detect abnormal prompts, which motivates us in our definition. Other works [40, 41, 46, 48] do not place an emphasis on probability. The *probability* condition is critical for analyzing memorization; as we will show later, any samples can be extracted from diffusion models, but not all are memorized.

4 RECOGNIZING IMAGE REPLICATION

We begin the measurement of memorization in diffusion models with a preliminary investigation on the recognition of image replication, which aims to decide the condition that a generated image x' replicates the target image x_0 (the *similarity* condition). Effective recognition is the basis for further measurement. Existing works adopted a "tiled" l_2 distance [8] or SSCD [40, 41] (a pre-trained model for copy detection) representations to calculate the similarity between x' and x_0 . Wen et al. [48]'s metric was designed to detect abnormal prompts and could not be used to identify a replication of x_0 . Nevertheless, to have an in-depth understanding of training image replication and accurate recognition, a more intrinsic and informative metric is necessary.

4.1 Methodology

Suppose that the input prompt is represented as $\varphi(e)$, where $e = [e_0, e_1, \dots, e_{N-1}]$ is a sequence of token embeddings and φ is a text encoder. To generate an image, a random Gaussian noise $\epsilon_0 \sim \mathcal{N}(0, I)$ is sampled and follows an iterative denoising process as introduced in Section 2.1. Besides the initial noise ϵ_0 , the vanilla sampling algorithm of diffusion models adds a different Gaussian noise at each step. Therefore, the generated image is determined by an array of noises. However, in practice more efficient samplers are utilized, e.g., DDIM sampler [42] and PLMS sampler [22], which only sample once at the beginning and then follow a deterministic denoising process. If the same initial noise is used, then the generated image will be exactly the same. We adopt DDIM sampler [42] in our experiments, therefore only consider the initial noise.

To recognize whether a noise-prompt pair (ϵ_0, e) can replicate the target image x_0 , we find it strongly correlated with the model's prediction error when we utilize ϵ_0 to blur $z_0 = \mathcal{E}(x_0)$. Instead of the default ϵ_0 -prediction error, we consider a more direct and effective z_0 -prediction error:

$$\mathcal{L}(x_0, \epsilon_0, e) = \mathbb{E}_t \left[\|z_0 - z_\theta(z_t, t, \varphi(e))\|_2^2 \right]$$

$$\begin{aligned} &= \mathbb{E}_t \left[\left\| z_0 - \frac{z_t - \sqrt{1 - \bar{\alpha}_t} \epsilon_\theta(z_t, t, \varphi(e))}{\sqrt{\bar{\alpha}_t}} \right\|_2^2 \right] \\ &= \mathbb{E}_t \left[\frac{1 - \bar{\alpha}_t}{\bar{\alpha}_t} \|\epsilon_0 - \epsilon_\theta(z_t, t, \varphi(e))\|_2^2 \right], \end{aligned} \quad (5)$$

where $z_t = \sqrt{\bar{\alpha}_t} z_0 + \sqrt{1 - \bar{\alpha}_t} \epsilon_0$. The z_0 -prediction error is equivalent to reweighted ϵ_0 -prediction error. The weight term $\frac{1 - \bar{\alpha}_t}{\bar{\alpha}_t}$ increases with larger t , which favors more accurate predictions in earlier sampling steps (later steps in the diffusion process correspond to earlier steps in the generation process). The intuition is that if the diffusion model can accurately predict z_0 out of ϵ_0 -blurred z_t at all steps (especially early sampling steps), then the sampling trace starting at ϵ_0 will head towards z_0 and finally generate $x_0 = \mathcal{D}(z_0)$. Note that $\mathcal{L}(x_0, \epsilon_0, e)$ only performs single-point detection (single noise ϵ_0 and single prompt e) and cannot be readily used to analyze memorization.

Aligning the starting point. In Stable Diffusion, the timestep schedule is discrete over a range (1000). The noisy image $z_T = \sqrt{\bar{\alpha}_T} z_0 + \sqrt{1 - \bar{\alpha}_T} \epsilon_0$ at the last step has minor difference from the Gaussian noise ϵ_0 , with Signal-to-Noise Ratio (SNR) of 0.0047. However, we have found that the minor difference could exert significant influence over the generation results, i.e., the generated images by z_T and ϵ_0 could be different. The gap between z_T and ϵ_0 is not constrained during diffusion model training; thus the behavior of ϵ_0 generation cannot be fully captured by the related loss function. To eliminate the inconsistency, we generate using $z_T = \sqrt{\bar{\alpha}_T} z_0 + \sqrt{1 - \bar{\alpha}_T} \epsilon_0$, a practice involved in image editing works [26]. This equals to sample from a biased Gaussian distribution $\mathcal{N}(\sqrt{\bar{\alpha}_T} z_0, (1 - \bar{\alpha}_T)I)$.

4.2 Experiment Setup

The correlation between our proposed metric $\mathcal{L}(x_0, \epsilon_0, e)$ and the replication of x_0 through (z_T, e) can be verified through a pair of bidirectional experiments.

4.2.1 The Ability of $\mathcal{L}(x_0, \epsilon_0, e)$ to Recognize Replication. This experiment evaluates that given a realistic dataset $\{(x_0^i, \epsilon_0^i, e^i, y^i)\}_{i=1}^M$, where $y^i = 1$ indicates replication and otherwise not, whether $\mathcal{L}(x_0, \epsilon_0, e)$ is able to accurately recognize replications.

We use Stable Diffusion V1.4 for evaluation. To build the dataset, we collect a set of 78 memorized image-prompt pairs found by Webster [46]. Each image is augmented with an additional BLIP [20] generated prompt. The BLIP-generated prompt provides adequate non-replication samples. This results in 156 image-prompt pairs. For each pair, we randomly sample 50 different Gaussian noises and then manually annotate y^i for each sample $(x_0^i, \epsilon_0^i, e^i)$. Finally, we build a dataset consisting of 7800 samples, where replication occurs in 3645 samples. An accurate estimation of $\mathcal{L}(x_0, \epsilon_0, e)$ requires a traversal of 1000 steps for Stable Diffusion. For efficiency, we uniformly sample 50 steps. Following Wen et al. [48], the detection performance is measured by Area Under Curve (AUC) of the Receiver Operating Characteristic (ROC) and the True Positive Rate at the False Positive Rate of 1% (TPR@1%FPR).

4.2.2 The Ability of $\mathcal{L}(x_0, \epsilon_0, e)$ to Generate Replication. The effectiveness of $\mathcal{L}(x_0, \epsilon_0, e)$ can also be presented in reverse. It can

Table 1: Recognition results of replication.

Metric	Sample Level		Image Level	
	AUC	TPR@1%FPR	AUC	TPR@1%FPR
Tiled l_2 [8]	0.999	0.973	1.000	1.000
SSCD [40, 41]	1.000	0.999	1.000	1.000
z_0 -prediction error	0.999	0.986	1.000	0.999

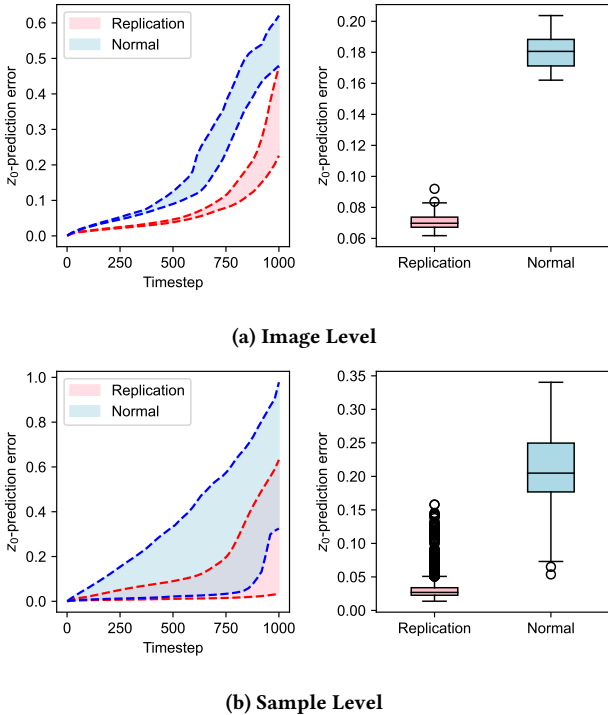


Figure 3: The z_0 -prediction error over each timesteps (left) and the distribution (right). (a) presents the error distribution of one example image.

be shown that a small level of $\mathcal{L}(x_0, \epsilon_0, e)$ is sufficient for generating replications. We study this effect in a tough setting. For the unmemorized (normal) images from LAION-Aesthetics V2 6.5+, a subset of Stable Diffusion’s training set with predicted aesthetics scores no less than 6.5, it is generally of low probability to sample an $\epsilon_0 \sim \mathcal{N}(0, I)$ that replicates x_0 [40]. However, we are able to invert a feasible ϵ_0^* that replicates the original x_0 by minimizing $\mathcal{L}(x_0, \epsilon_0, e)$,

$$\epsilon_0^* = \arg \min_{\epsilon_0} \mathcal{L}(x_0, \epsilon_0, e). \quad (6)$$

The ability of $\mathcal{L}(x_0, \epsilon_0, e)$ to trigger a rare event yields strong evidence for its correlation with replication. For all experiments, we use the Adam optimizer with an initial learning rate of 0.1 and without weight decay. We use a batch size of 32 (timesteps) and train for a total of 1K iterations.

4.3 Results

4.3.1 The Ability of $\mathcal{L}(x_0, \epsilon_0, e)$ to Recognize Replication. The performance is evaluated in sample-level and image-level. The sample-level takes the 7800 samples all together for evaluation. The Image-level evaluation calculates AUC and TPR@1%FPR respectively for each image and average them. Table 1 presents the recognition results. All the metrics achieve almost perfect performance. Figure 3 shows the distribution of $\mathcal{L}(x_0, \epsilon_0, e)$ for replication samples and normal ones. For each individual sample, there is a clear margin between replication and normal samples across most timesteps (Figure 3a), particularly in later steps. While sample-level distribution shows a large overlap between replication and normal samples (Figure 3b). This indicates that there is not a universal criterion for recognizing replication for all images. What’s more, the normal samples present z_0 -prediction error with a larger variance (Figure 3 right), which indicates that the normally generated images are more diversified than the memorized generations.

4.3.2 The Ability of $\mathcal{L}(x_0, \epsilon_0, e)$ to Generate Replication. We invert the initial noise ϵ_0 for each image with different input prompts, including their training caption, a BLIP-generate caption and an empty string. As shown in Figure 4, for either memorized training images or randomly sampled normal images, for either original training captions, BLIP-generated new captions or empty captions, minimizing $\mathcal{L}(x_0, \epsilon_0, e)$ produces successful inversion of the input noise ϵ_0 that leads to replication of x_0 . It demonstrates that $\mathcal{L}(x_0, \epsilon_0, e)$ is a strong indicator for training image replication. Compared to normal images, the inversion for memorized images presents relatively more authentic reconstruction, which indicates that memorized images are easier to replicate.

Condition 1: similarity. The z_0 -prediction error meets the *similarity* condition. We directly utilize internal prediction errors of diffusion models as an indicator of the similarity between the generated image and target image. We believe that based on the model’s own function for comparison is more reliable than using a coarse metric [8] or external independently trained models [40, 41].

5 TRIGGER THE MEMORIZATION

Recognizing image replication works after the deployment of diffusion models to prevent possible leakage of training images. The developers of an image generation model also have strong motivation to perform safety analysis on a target set of sensitive images during development of their model. This acts as a proactive defense against memorization. The main goal of the safety analysis against memorization is to determine whether the target images are memorized and to measure the extent to which they are memorized. As a straightforward approach, searching for prompts that are prone to generate the target images is not feasible for safety measurement because it is random and laborious. Instead, we propose an inversion-based analysis without the need to access any prompts.

The safety analysis against memorization is accomplished in two steps. First, for each target image, we attempt to invert an input prompt that triggers the model’s memorization behavior on it. We verify by contradiction that if an image is safe, then it is impossible to invert a prompt that triggers its memorization. Second, we perform an analysis on the unconditional diffusion model and find that the unconditional diffusion model trained on

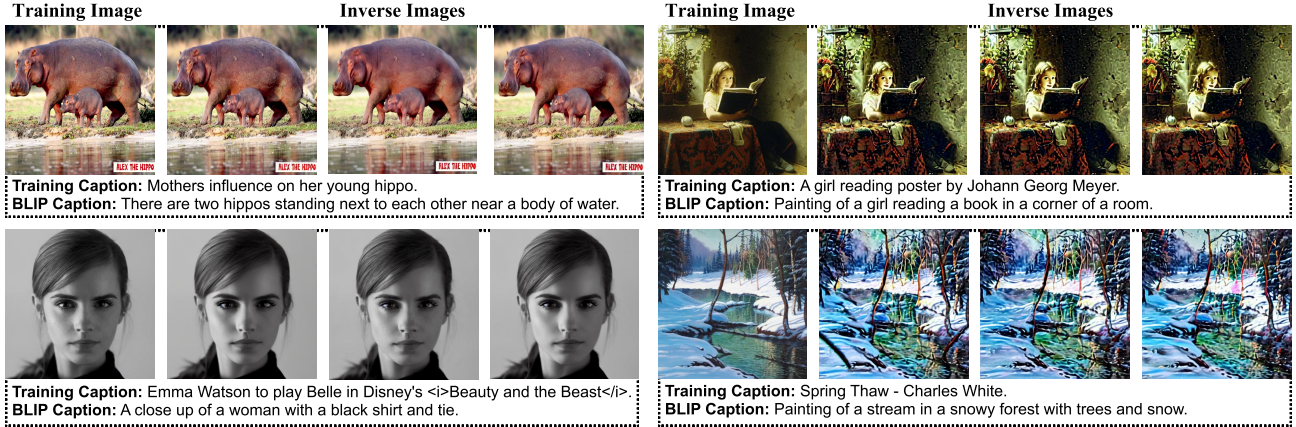


Figure 4: The results of noise inversion for memorized images (left) and normal images (right). In each block, the leftmost image is the training image. The right three are generated images using inverted noises, along with training caption, BLIP-generated caption and an empty string "". Overall, each image can be successfully inverted by minimizing the z_0 -prediction error, while memorized images are easier to invert and of higher fidelity.

large-scale data is safe from memorization. It thus serves as a guard for measuring the safety of the conditional text-to-image model.

In this section, we elaborate how to trigger the memorization of an image. The measurement of memorization is described in the next section.

5.1 Methodology

To answer the question that if a target image could be memorized, we attempt to search for a prompt that triggers the generation of the target image. This can be done by minimizing the expectation of conditional prediction error with respect to the input token embeddings e ,

$$e^* = \arg \min_e \mathbb{E}_{\epsilon_0 \sim \mathcal{N}(0, I)} [\mathcal{L}(x_0, \epsilon_0, e)]. \quad (7)$$

However, this straightforward prompt inversion causes overestimation of memorization. Indeed, we are always able to invert an optimal e^* that reduces the prediction error of any target image x_0 to a desired low level. As a result, the image appears to be "memorized". This is because the pre-trained vocabulary embeddings \mathcal{V} only distribute as a finite number of spots in the infinite large embedding space. A valid e^* that reflects the memorization of x_0 should not only lead to a low level of prediction error but also be close to the manifold of vocabulary embeddings \mathcal{V} . The condition can be fulfilled by adding a regularizer $\mathcal{R}(e, \mathcal{V})$ to Equation 7,

$$e^* = \arg \min_e \mathbb{E}_{\epsilon_0 \sim \mathcal{N}(0, I)} [\mathcal{L}(x_0, \epsilon_0, e)] + \lambda \mathcal{R}(e, \mathcal{V}), \quad (8)$$

where λ is a hyperparameter to control the weight of regularizer.

Condition 2: existence. The regularizer meets the *existence* condition. It works as an adversary to the expectation of conditional prediction error: A target image x_0 is memorized if and only if the contradiction between them can be solved. If the regularized objective is not optimizable for a target image, then we can claim that the image is safe from memorization. The reliability of making

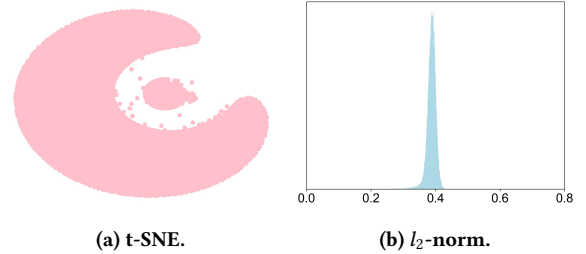


Figure 5: Pre-trained token embeddings do not present a regular distribution.

such a claim is established on the trust in the optimizers utilized to minimize Equation 8. For deep neural networks, we believe that modern optimizers [18, 23] are capable of taking responsibility.

It is challenging to accurately constrain the distance of token embeddings e to the manifold of pre-trained vocabulary embeddings, because the pre-trained vocabulary embeddings do not present a regular distribution, as shown in Figure 5a for CLIP (CLIP is used as the text encoder of Stable Diffusion). We devise two regularizers that constrain the l_2 -norm of optimized token embeddings ϵ^* . This is motivated by the observation that minimizing the prediction error without regularization for normal images typically produces token embeddings with sufficiently large l_2 -norm. Therefore, the first regularizer equals an l_2 -norm regularizer $\mathcal{R}_1(e, \mathcal{V}) = \|e\|_2^2$. \mathcal{R}_1 seems irrelevant to the vocabulary \mathcal{V} but takes advantage of the fact that pre-trained vocabulary embeddings have relatively small l_2 -norm (see Figure 5b). Another regularizer \mathcal{R}_2 adds a term to \mathcal{R}_1 that encourages the learned token embeddings to be as close to any of the pre-trained vocabulary embeddings as possible,

$$\mathcal{R}_2(e, \mathcal{V}) = \|e\|_2^2 + \frac{1}{N} \sum_{i=0}^{N-1} \mathcal{H}(e_i, \mathcal{V}), \quad (9)$$

where $\mathcal{H}(e_i, \mathcal{V})$ is the entropy calculated over the probabilistic distribution on the inner-product distance between i -th token and the vocabulary. This regularizer enables to search for realistic hard prompts.

5.2 Experiment Setup

We use the 78 memorized images and 100 randomly sampled normal images from LAION as the target image set. For all experiments, we do not access training captions of the target images. We use the Adam optimizer with an initial learning rate of 0.01 without decay. The l_2 -norm regularization is implemented by Adam’s inner weight decay. λ is set to 0.01. We use a batch size of 16 and optimize for a total of 500 iterations. Each image is resized and center cropped to 512×512 without augmentations.

5.3 Results

Note that a prompt e is composed of N token embeddings, each of which represents a token. Stable Diffusion’s text encoder by default uses a maximum length of 77 tokens, in which the first and last tokens are padded tokens indicating the start and end of a prompt. The rest 75 tokens are free to optimize.



Figure 6: Examples of generated images using optimized token embeddings. 4 images are randomly generated for each optimization and all examples present the problem of memorization. The last row exhibits an example of partial memorization, where not all generations collapse to the same image.

Through adjusting the number of tokens to optimize from 1 to 75, we find that out of the 78 memorized images discovered by Webster [46], the memorization of 66 images can be triggered by optimizing only 1 token, 2 images can be triggered by optimizing 2 tokens, the other 10 images are only partially memorized images, no matter how many tokens are optimized, as illustrated in Figure 6. In contrast, the memorization of normal images cannot be triggered with regularization. Figure 7 shows training statistics of memorized images and normal images, it can be seen that the prediction error and regularization term can be simultaneously optimized to small values for memorized images. In contrast, for normal images, only the l_2 -norm of token embeddings is minimized, while the prediction error of normal images remains high. It demonstrates that for

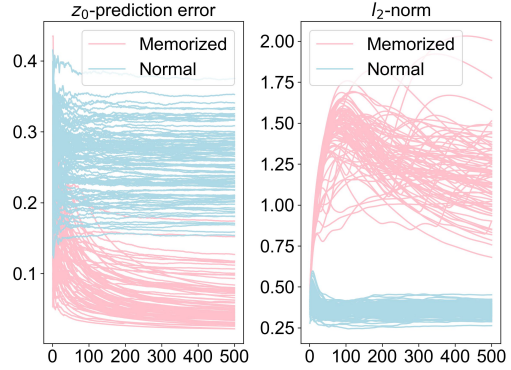


Figure 7: z_0 -prediction errors and l_2 -norm of token embeddings during training time. Memorized images present low values for both prediction errors and l_2 -norm of token embeddings at the end of training. Prompt inversion for normal images can only optimize the l_2 -norm of token embeddings while prediction errors remain high across the whole training process.

Algorithm 1 Hard prompt inversion for memorization.

Input: the target image x_0 , encoder \mathcal{E} , token embeddings $e = [e_0, e_1, \dots, e_{N-1}]$, vocabulary embeddings \mathcal{V} , weight λ , number of candidate tokens k , optimization steps M , batch size B , learning rate γ , timesteps T in diffusion model

Output: optimal hard prompt $\hat{t} = [\hat{t}_0, \hat{t}_1, \dots, \hat{t}_{N-1}]$

```

 $z_0 = \mathcal{E}(x_0)$ 
 $err = +\infty$ 
for  $i = 1$  to  $M$  do
  sample  $B \epsilon \sim \mathcal{N}(0, I), t \sim U(1, T)$ 
   $z_t = \sqrt{\alpha_t} z_0 + \sqrt{1 - \alpha_t} \epsilon$ 
   $g = \nabla_e \mathcal{L}(z_t, t, e) + \mathcal{R}_2(e, \mathcal{V})$ 
   $e = e - \gamma g$ 
end for
Sample a test set  $\epsilon \sim \mathcal{N}(0, I), t \sim U(1, T)$ 
 $z_t = \sqrt{\alpha_t} z_0 + \sqrt{1 - \alpha_t} \epsilon$ 
for  $[t_0, t_1, \dots, t_{N-1}] \in \text{top-}k(e_0 \mathcal{V}^T) \times \text{top-}k(e_1 \mathcal{V}^T) \times \dots \times \text{top-}k(e_{N-1} \mathcal{V}^T)$  do
   $e' = \mathcal{V}(t_0, t_1, \dots, t_{N-1})$ 
  if  $\mathcal{L}(z_t, t, e') < err$  then
     $\hat{t} = [t_0, t_1, \dots, t_{N-1}]$ 
  end if
end for

return  $\hat{t}$ 

```

normal (unmemorized) images, the contradiction between reducing prediction errors and aligning the learned tokens to the pre-trained tokens is unsolvable. Therefore, for the target images to protect, if we cannot optimize token embeddings that follows the pre-trained token embedding distribution to reduce the prediction error, then we can claim that the images are not memorized.

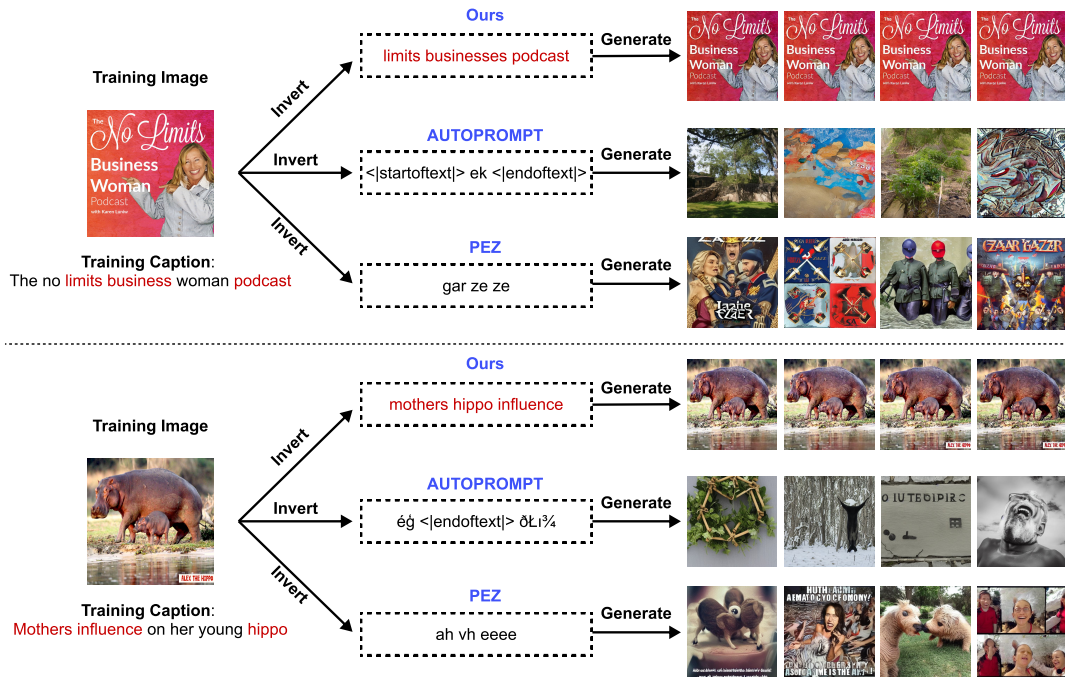


Figure 8: Results of hard prompt inversion for memorized images. Our inversion algorithm is able to invert an training image to a prompt that triggers its memorization. Existing hard prompt tuning methods AUTOPROMPT and PEZ are not effective in analyzing memorization.

For the valid token embeddings that successfully trigger the memorization of some images, there is still a gap between the learned continuous token embeddings and discrete tokens. Simple regularizer, e.g., l_2 -norm regularizer as we used, does not provide a guarantee that the learning continuous token embeddings can be projected to realistic tokens. This is challenging because there are infinite number of points in the continuous embedding space, a subset of which have lower error than a possible hard prompt. The token embeddings could be over-optimized to areas that produce lower error but do not correspond to any tokens prompts. What’s more, existing hard prompt tuning methods based on greedy algorithm are not applicable to search prompts that trigger the memorization of target images, because we have observed that prompts that trigger memorization do not necessarily have greedy property.

To solve the problem, we propose a simple but effective algorithm to optimize hard prompts that trigger memorization, as in Algorithm 1. Algorithm 1 performs brute-force search in the Cartesian product of N sets, each of which contains k candidate tokens with smallest distance to the learned token embeddings. The optimal prompt is the one with minimal prediction error. The effectiveness of the algorithm heavily relies on the initialization, a common problem in hard prompt tuning [38, 47]. We repeat Algorithm 1 for a maximum of 20 runs with different initialization. We compare our algorithm with two hard prompt tuning algorithms AUTOPROMPT [38] and PEZ [47]. The number of tokens to optimize is set to 3. For the 20 inverted prompts, we choose the one with

the lowest prediction error for illustration. Figure 8 illustrates 2 successful inversions.

Our hard prompt inversion algorithm successfully inverts a prompt that trigger the memorization. It reflects that the memorization is only determined by a few key tokens (3 tokens in the example). It also reflects that the prompts that cause training image replication are not unique. The positions of the key tokens could be different. As shown in the example, the three words "limits", "business" and "podcast" are respectively the 3rd, 4th and 6th. It has no influence to shift them to the head of the prompt, as inverted by us. However, the order of tokens does not always have no effect. Permuting the prompt to "businesses limits podcast" would fail to trigger memorization. This explains why the hard prompt inversion is sensitive to initialization states. It is hard to constrain the position of inverted tokens simply by gradient descent. In contrast, AUTOPROMPT and PEZ do not work in prompt inversion for memorization. It demonstrates that inverting prompt for memorization is more difficult than semantic understanding tasks as their original applications. We have observed that the prompts that trigger memorization does not have greedy-solvable property, therefore they cannot be found by AUTOPROMPT and PEZ. Specifically, we initialize the prompt to "limits business <|endoftext|>" for AUTOPROMPT and PEZ, and run them to search for the third token "podcast". If it is greedy-solvable, AUTOPROMPT and PEZ would leave the first two words unchanged and find the last word "podcast". However, they gradually change the first two words and do not converge.

Due to the dilemma, continuous token embeddings are adopted in subsequent measurement. Although the continuous token embeddings do not strictly meet the *existence* condition for potential memorized images, we would like to clarify that it is reasonable to use them for measurement for two reasons. Firstly, for potential memorized images, continuous token embeddings inverted with regularization are sufficient to indicate that memorization has happened. Secondly, for normal images, it is meaningless to invert hard prompts for them. Projecting the optimized token embeddings to hard prompts anyway will introduce additional error into measurement.

6 MEASURE THE MEMORIZATION

We have discussed how to recognize the replication of a training image x_0 given a pair of noise and prompt (ϵ_0, e) , and how to verify the existence of a prompt to trigger memorization of a training image. In this section, we focus on the measurement of memorization and describe how the measurement meets the last *probability* condition.

Given previous results, an intuitive method to measure the memorization would be first determining a threshold of the z_0 -prediction error $\mathcal{L}(x_0, \epsilon_0, e)$ (Section 4) for recognizing replications and then estimate the probability of that $\mathcal{L}(x_0, \epsilon_0, e)$ is no larger than the threshold when the inverted prompt e^* (Section 5) is input. However, the intuitive method is difficult to implement. As demonstrated by Figure 3, there is not a universal threshold applicable to every image, hence a unique threshold must be determined for each image. To accurately locate the threshold, we can either take the upper bound of $\mathcal{L}(x_0, \epsilon_0, e^*)$ or the lower bound of $\mathcal{L}(x_0, \epsilon_0, e)$ for all normal prompts e . Both options are difficult to implement, because the upper bound of $\mathcal{L}(x_0, \epsilon_0, e^*)$ is prone to overestimation (not strictly l_2 bounded) and the lower bound of $\mathcal{L}(x_0, \epsilon_0, e)$ requires to evaluate all potential prompts, which is laborious.

Instead, we avoid deciding the boundary of replication and novel generation but propose an indirect measurement of memorization by comparing the distribution of $\mathcal{L}(x_0, \epsilon_0, e^*)$ to the distribution of a safe model. Then the measurement of memorization equals how much threat an inverted prompt has introduced into the safe model. Motivated by previous observations [40], we find the unconditional diffusion model trained on large-scale data is safe from memorization and thus could be utilized as the safe model. For the remainder of this section, we first verify the safety of unconditional diffusion model and then describe the measurement.

6.1 Unconditional Model

The unconditional model is part of the text-to-image model and used as penalty at sampling time (see Section 2.2). It can be safe from memorization for the following reasons. First, the unconditional model is trained to maximize the likelihood of data distribution without any outer guidance (empty string in Stable Diffusion). The memorization can only happen when the unconditional model frequently generates a certain image, a form of representation space collapse. However, one of the advantages of diffusion models is its stability in training, where no collapse is discovered. Second, under the observation that memorization is caused by overfitting to an image-prompt pair [41], the unconditional model has no chance to



Figure 9: Results of noise inversion for memorized images in Stable Diffusion. Left: training image. Middle: generated image without regularization. Right: generated image with regularization. Even with regularization, memorized images can be successfully inverted.

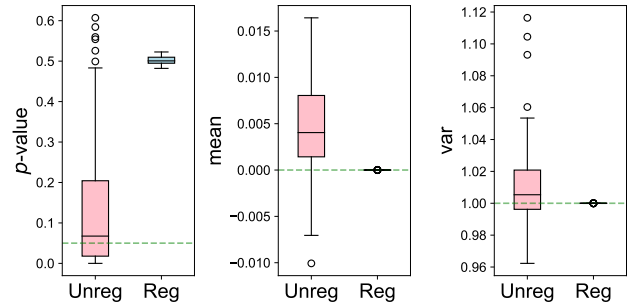


Figure 10: The distribution of p -value, mean and variance of noises inverted for memorized images in Stable Diffusion using their training captions. The minimum p -value and desired values of mean and variance are plotted in green dashed line. Without regularization, straightforward noise inversion caused the inverted noises far from the standard Gaussian distribution. The regularized noise inversion successfully circumvent the over-optimization problem. Unreg: Unregularized, Reg: Regularized.

overfit because its training data consists of image-null pairs which forms a many-to-one correspondence. Last, Somepalli et al. [40] have found that when the number of training data is large enough, unconditional diffusion models would not replicate training images, but only generate similar ones.

6.1.1 Methodology. It is intractable to estimate the probability that the model replicates x_0 as it requires to find all the potential ϵ_0^* and accumulate the probability within their "exactly alike" boundary. Therefore, it is impossible to estimate the safety of unconditional diffusion models directly by probability. We verify the safety of unconditional diffusion models against memorization by contradiction based on noise inversion that replicate a target image x (Equation 6). In practice, it was shown that massive sampling from $\mathcal{N}(0, I)$ to generate x for the unconditional model does not work [40]. Noise inversion seems to provide an approach, but we will demonstrate



Figure 11: Results of noise inversion in unconditional Stable Diffusion and a diffusion model trained on FFHQ. Each block contains three images: left: training image, middle: generated image without regularization, right: generated image with regularization. For unconditional models, the training images, even memorized ones, cannot be replicated with normality regularization, which means that unconditional models have little probability of memorizing their training data.

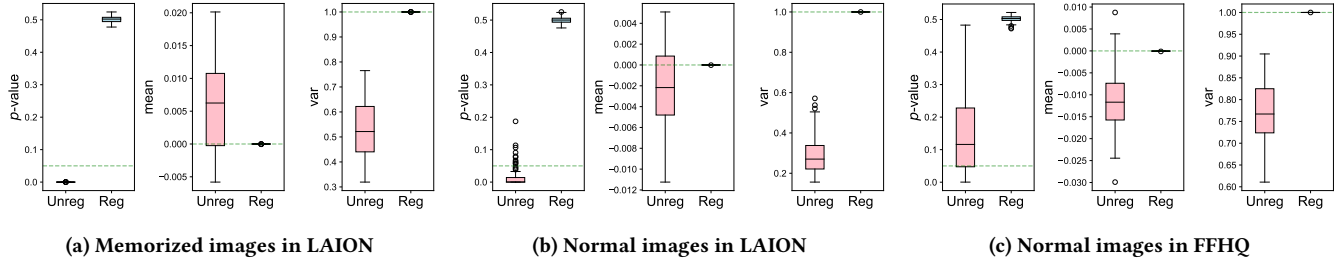


Figure 12: Unconditional models' distribution of p -value, mean and variance of inverted noises. Memorized images in text-to-image Stable Diffusion can not be replicated by its unconditional part.

that noises found by this way are impossible to be drawn from $\mathcal{N}(0, I)$.

Directly minimizing $\mathcal{L}(x, \epsilon)$ leads to over-optimization: Even for memorized image-prompt pairs, the noise ϵ^* obtained by minimizing $\mathcal{L}(x, \epsilon)$ are away from $\mathcal{N}(0, I)$, indeed there are a wealth of normal noises (noises that are likely drawn from $\mathcal{N}(0, I)$) available. It becomes confusing for our verification whether there exist normal noises that will replicate x . If there exist, we might just over-optimize and miss them. To avoid this interference factor, we assume that the noise ϵ to be optimized is drawn from another Gaussian distribution $\mathcal{N}(\mu, \sigma^2)$ with parameters μ and σ^2 . Motivated by the prior matching in Variational AutoEncoder (VAE) [19], we invert μ and σ^2 with an regularized objective:

$$\begin{aligned} \mu^*, (\sigma^2)^* &= \arg \min_{\mu, \sigma^2} \mathbb{E}_{\epsilon \sim \mathcal{N}(0, I)} [\mathcal{L}(x, \mu + \sigma\epsilon)] \\ &\quad + D_{KL}(\mathcal{N}(\mu, \sigma^2) \| \mathcal{N}(0, I)), \\ D_{KL}(\mathcal{N}(\mu, \sigma^2) \| \mathcal{N}(0, I)) &= \frac{1}{2} \sum_i (\mu_i^2 + \sigma_i^2 - \log \sigma_i^2 - 1). \end{aligned} \quad (10)$$

The regularization term calculates the distance between the Gaussian distribution where the noise is drawn and the standard Gaussian distribution. Through this reparameterization trick, we do not directly optimize ϵ but the distribution it follows. In this way, the prediction error of the diffusion model $\mathcal{L}(x, \mu + \sigma\epsilon)$ and the regularization term become two adversaries. The contradiction between them can be solved iff noises drawn from a distribution

close to the standard Gaussian distribution have low prediction errors (indicating memorization) simultaneously.

This constraint can be satisfied by the memorized image-prompt pairs in conditional text-to-image models, as shown in experiments. However, for unconditional models, it cannot be solved, which demonstrates that unconditional models are safe from memorization.

6.1.2 Experiment Setup. Apart from Stable Diffusion's unconditional model, we additionally investigate an unconditional diffusion model trained on the human face dataset FFHQ [17, 32] consisting of 70000 images. For Stable Diffusion, we perform the noise inversion for the 78 memorized images and 100 normal images randomly sampled from its training set. The input prompt is fixed to an empty string. For the model trained on FFHQ, 100 randomly sampled training images are used for experiments. We perform the Kolmogorov-Smirnov hypothesis test (KS test) on the optimized $\epsilon^* \sim \mathcal{N}(\mu^*, (\sigma^2)^*)$ to decide whether ϵ^* can be drawn from a standard Gaussian distribution. The null hypothesis is set to " ϵ^* is drawn from a standard Gaussian distribution" and the p -value is set to 0.05 for all experiments. In a Kolmogorov-Smirnov test, if the calculated p -value is less than 0.05, the null hypothesis should be rejected and otherwise accepted. For each learned Gaussian distribution $\mathcal{N}(\mu^*, (\sigma^2)^*)$, we randomly sample 1000 samples from it and take the average p -value over the 1000 samples. For optimization, Adam optimizer is used with an initial learning rate of 0.1 following cosine

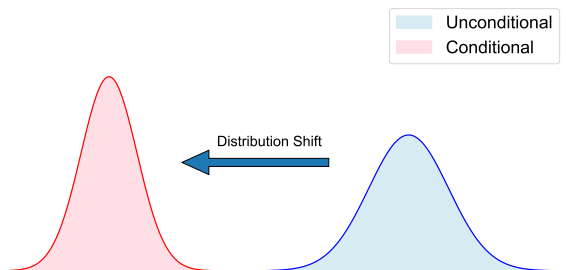


Figure 13: The introduction of a prompt shifts the unconditional error distribution.

decay without weight decay. We use a batch size of 32 and train for a total of 500 iterations.

6.1.3 Results. We first demonstrate the effectiveness of our regularized noise inversion (Equation 10) to circumvent over-optimization through a study on memorized images in Stable Diffusion. For each image, we adopt their training prompt that will trigger memorization. Figure 9 shows the generation results using optimized noise ϵ^* . Whether regularized or not, memorized images are easy to reproduce. Figure 10 exhibits the p -value, mean and variance of the inverted noises by unregularized (Equation 6) and regularized (Equation 10) optimizations. It can be observed that inversion via our regularized objective produces normally distributed noises with high p -value of KS test, zero mean and unit variance. It effectively circumvents the over-optimization problem, which can be then utilized to measure the safety of unconditional models.

For unconditional models, we perform noise inversion using Equation 10, with or without the KL-divergence regularization term. The results can be found in Figures 11 and 12. For unconditional models, it fails to reproduce training images on both models when the normality of noises is constrained. However, without normality regularization, as in Figure 12, the optimized noises present lower p -values, which indicates that they cannot be drawn from the standard Gaussian distribution with high probability. The results demonstrate that unconditional models are more safe to protect their training images from replication. Note that compared to Stable Diffusion trained on LAION, the diffusion model trained on FFHQ presents better normality for the inverted noises. This might be attributed to its limited number of training data (70000) embedded into a large latent space $\mathcal{R}^{3 \times 64 \times 64}$. In contrast, Stable Diffusion is trained on 2 billions of data with a slightly larger latent space $\mathcal{R}^{4 \times 64 \times 64}$. The large contrast between the number of training data and the dimensionality of latent space "leaves more space to memorize one instance", which can be observed in Figure 12c that noises inverted on FFHQ tend to have larger variance than those on LAION.

6.2 Measurement

6.2.1 Methodology. As discussed in Section 6.1, unconditional diffusion model trained on large-scale data is safe from memorization. Therefore, the unconditional error $\mathcal{L}(x_0, \epsilon_0)$ represents a safe distribution when ϵ_0 is sampled from the standard Gaussian distribution.

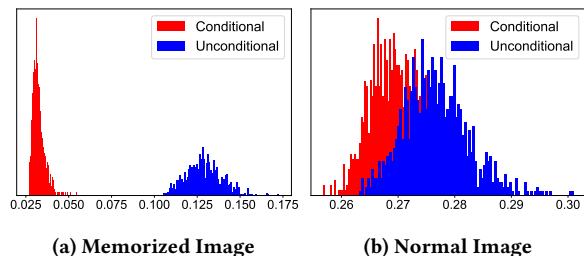


Figure 14: Example of prediction error distributions for a memorized image and a normal image in Stable Diffusion.

It can then serve as a guard to measure the safety against memorization of any conditional error distribution $\mathcal{L}(x_0, \epsilon_0, e)$ when some prompt e is introduced. We consider the worst-case conditional error distribution $\mathcal{L}(x_0, \epsilon_0, e^*)$ where e^* is obtained through Equation 8. We then measure the extent to which x_0 is memorized as the distribution shift of prediction errors from unconditional to the worst-case conditional, as illustrated in Figure 13.

Distribution shift. The distribution shift can be calculated by the Wasserstein distance between unconditional error distribution and the worst-case conditional error distribution. Wasserstein distance measures the minimal cost to convert unconditional error distribution to conditional error distribution. Wasserstein distance is suitable for measurement of memorization because it takes into consideration the amount of errors that are lowered by introducing a prompt. The larger the Wasserstein distance is, the lower the prediction error has been reduced, and to more extent the target image is memorized. We denote the measure by $\mathcal{M}(x_0)$. The distributions of $\mathcal{L}(x_0, \epsilon_0)$ and $\mathcal{L}(x_0, \epsilon_0, e^*)$ are estimated using the Monte Carlo method.

Condition 3: probability. The measurement based on the distribution shift meets the *probability* condition of memorization. We do not directly calculate the probability of memorization but calculate a correlated measure by referring to the safe unconditional model. Through this way, we avoid to determine an absolute threshold to distinguish between replicating and normal generations. According to Chebyshev's inequality, the probability that unconditional prediction errors deviates from its mean by more than $k\sigma$ is at most $1/k^2$. Therefore, when a prompt is input instead of an empty string, the larger the distribution of the prediction errors is shifted towards the original rare case, the more probable that memorization has been triggered.

6.2.2 Experiment Setup. Based on the prompt inversion results, the extent to which a target image is memorized $\mathcal{M}(x_0)$ can be estimated by the Wasserstein distance between the unconditional error distribution $\mathcal{L}(x_0, \epsilon_0)$ and worst-case conditional error distribution $\mathcal{L}(x_0, \epsilon_0, e^*)$. For any image, we invert a sequence of token embeddings e^* as in Equation 8. All the 75 free tokens are optimized. We calculate $\mathcal{M}(x_0)$ for the 78 memorized images and 100 randomly sampled normal images. 1000 Gaussian noises are randomly sampled to estimate each error distribution. The probability density function is calculated with 2000 bins over the range $[0, 0.4]$.

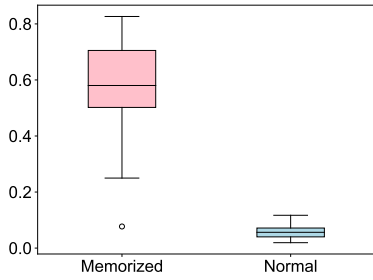


Figure 15: Memorization measured by Wasserstein distance for memorized images and normal images. Memorized images present a significant higher level of memorization.



Figure 16: Examples of images that are memorized to relatively smaller extent. Original training images are in the first column.

6.2.3 Results. Figure 14 shows an example of the prediction error distribution for both memorized and normal images. The conditional error distribution of memorized images shows an obvious gap to the unconditional error distribution. However, the conditional error distribution of normal images get entangled in its unconditional error distribution. Figure 15 illustrates the Wasserstein distance distribution of all test images. Memorized images present significantly larger Wasserstein distances compared to normal images.

Recall that there are partially memorized images in the test set. We find that these images correspond to lower distance compared to other completely memorized images, as shown in Figure 16. This demonstrates the effectiveness of our measurement to quantify the extent to which an image is memorized beyond simply distinguishing memorized images from normal ones.

7 RELATED WORK

7.1 Memorization in Image Generation Models

Memorization has previously raised concerns in image generation models, e.g., GAN and VAE, mainly focusing on the type of unconditional generation. There have been studies on training algorithm [34] and evaluation metric [13] to improve the generalization ability of GANs to get rid of simply copying from training data. It has been shown that small data size [10] or too longer training [43] can cause memorization in GANs. Van der Burg et al. [44] measure

memorization in VAE as the changed probability when removing one sample from the training set.

For diffusion models, Vyas et al. [45] propose a copyright protection method to prevent replication of sensitive training images. The model is trained to match a safe model that does not take sensitive data for training. Carlini et al [8] and Somepalli et al. [40, 41] demonstrates that memorization also occur in text-to-image diffusion models. Memorized images are found from numerous generated samples by membership inference attack or searching for the most similar training images using image retrieval models. Webster [46] provides more efficient attacks to extract training images from text-to-image models. Subsequently, Wen et al. [48] focus on the detection of abnormal prompts that will trigger generation of training images. Compared to these works, we perform a practical analysis on training image memorization with no need to access any prompts. Our analysis not only is able to find memorized images, but also provides quantitative measurement and allows developers to claim safety on normal images.

7.2 Inversion of Diffusion Models

Inversion techniques in diffusion models are widely studied mainly for image editing [11, 26, 52]. Through inversion, the object, style and concept contained in the source images can be compressed in latent noises or input token embeddings. Then the inverted latent noises or input token embeddings are utilized to generate novel images that preserve the desired content.

We leverage analogous inversion techniques to analyze training image memorization in diffusion models. Instead of utility, we focus more on the regularity of inverted signals, which is essential to identify memorized images. In this sense, memorized images are a class that is "naturally" invertible.

8 DISCUSSION AND CONCLUSION

In this work, we perform a practical analysis on memorization in text-to-image diffusion models. Our analysis targets a set of images and measures the extent to which they are memorized, without the need to collect massive prompts. We first provide a formal definition of training image memorization and identify three conditions to say an image is memorized. We show that the model's internal prediction error is a strong indicator for training image replication. Based on it, the existence of a prompt that triggers memorization is analyzed by inverting an array of token embeddings. We highlight the importance of regularization in inversion-based verification. Furthermore, we propose a regularized noise inversion method to verify that the unconditional diffusion models trained on large-scale data are safe from memorization. Based on the verification, the extent to which an image is memorized is measured by the distribution shift between unconditional error and conditional error. In practice, developers of text-to-image diffusion models can leverage our analysis method to perform safety analysis on a set of sensitive training images. Our method enables developers to discover potential memorization risks and fix them timely or to responsibly claim safety against memorization to their data providers. We study the security of training data in diffusion models in terms of memorization. In the future, analysis on wider scopes is also in urgent need.

Defense against unsafe derivative generation. A majority of generated images by diffusion models are more than copies of training images, which is called derivative generation. Among them, considerable ethical threats have been found [2, 25, 28], including bias, pornography, violence, etc. Through editing methods and several pieces of images, diffusion models can also be used to generate variants of personal human photos [11] and imitate artists' works [21, 37]. In the past, a large portion of efforts to circumvent unsafe generation are put into training data cleaning [2, 5] and toxic content detection. Nonetheless, it is still possible to induce them by visual synonyms [2] or seemingly innocuous prompts [51]. Towards more reliable defense against unsafe derivative generation, improving interpretability of diffusion models' latent space would be beneficial. We haven't had a full understanding of the semantic structure of diffusion models' latent space yet [50]. Devising training algorithms that align human ethical notions to diffusion models' latent space would be an interesting direction.

Limitations. Our work has two limitations. First, although our hard prompt inversion algorithm is more effective than existing hard prompt tuning methods in analyzing memorization, it does not work for all memorized images, especially those requiring more key tokens to trigger. In practice, it would provide stronger evidence if an example hard prompt is available. We hope stable and effective hard prompt inversion algorithms for analyzing memorization can be devised. Second, we only provide security analysis method for unconditional and text-to-image diffusion models. A more comprehensive investigation for other type of conditional models and corresponding regularization methods should also be conducted. Despite the limitations, we believe our method provides a practical security analysis tool for developers to optimize their models.

REFERENCES

- [1] Artist finds private medical record photos in popular AI training data set. <https://arstechnica.com/information-technology/2022/09/artist-finds-private-medical-record-photos-in-popular-ai-training-data-set/>.
- [2] DALL-E 2 pre-training mitigations. <https://openai.com/research/dall-e-2-pre-training-mitigations>
- [3] DALL-E 3. <https://openai.com/dall-e-3>
- [4] Midjourney. <https://www.midjourney.com>
- [5] Safety Review for LAION 5B. <https://laion.ai/notes/laion-maintenance/>
- [6] Martin Arjovsky, Soumith Chintala, and Léon Bottou. 2017. Wasserstein GAN. *CoRR* abs/1701.07875 (2017). arXiv:1701.07875 <http://arxiv.org/abs/1701.07875>
- [7] Tim Brooks, Bill Peebles, Connor Holmes, Will DePue, Yufei Guo, Li Jing, David Schnurr, Joe Taylor, Troy Luhman, Eric Luhman, Clarence Ng, Ricky Wang, and Aditya Ramesh. 2024. Video generation models as world simulators. <https://openai.com/research/video-generation-models-as-world-simulators>
- [8] Nicholas Carlini, Jamie Hayes, Milad Nasr, Matthew Jagielski, Vikash Sehwal, Florian Tramèr, Borja Balle, Daphne Ippolito, and Eric Wallace. 2023. Extracting Training Data from Diffusion Models. In *32nd USENIX Security Symposium, USENIX Security 2023, Anaheim, CA, USA, August 9-11, 2023*, Joseph A. Calandrino and Carmela Troncoso (Eds.). USENIX Association, 5253–5270. <https://www.usenix.org/conference/usenixsecurity23/presentation/carlini>
- [9] Prafulla Dhariwal and Alexander Quinn Nichol. 2021. Diffusion Models Beat GANs on Image Synthesis. In *Advances in Neural Information Processing Systems 34: Annual Conference on Neural Information Processing Systems 2021, NeurIPS 2021, December 6-14, 2021, virtual*, Marc'Aurelio Ranzato, Alina Beygelzimer, Yann N. Dauphin, Percy Liang, and Jennifer Wortman Vaughan (Eds.), 8780–8794. <https://proceedings.neurips.cc/paper/2021/hash/49ad23d1ec9fa4bd8d77d02681df5cfa-Abstract.html>
- [10] Qianli Feng, Chenqi Guo, Fabian Benitez-Quiroz, and Aleix M. Martinez. 2021. When do GANs replicate? On the choice of dataset size. In *2021 IEEE/CVF International Conference on Computer Vision, ICCV 2021, Montreal, QC, Canada, October 10-17, 2021*. IEEE, 6681–6690. <https://doi.org/10.1109/ICCV48922.2021.00663>
- [11] Rinon Gal, Yuval Alaluf, Yuval Atzmon, Or Patashnik, Amit Haim Bermano, Gal Chechik, and Daniel Cohen-Or. 2023. An Image is Worth One Word: Personalizing Text-to-Image Generation using Textual Inversion. In *The Eleventh International Conference on Learning Representations, ICLR 2023, Kigali, Rwanda, May 1-5, 2023*. OpenReview.net. <https://openreview.net/pdf?id=NAQvF08TcyG>
- [12] Andres Guadamuz. Photographer sues LAION for copyright infringement. <https://www.technollama.co.uk/photographer-sues-laion-for-copyright-infringement>.
- [13] Ishaan Gulrajani, Colin Raffel, and Luke Metz. 2019. Towards GAN Benchmarks Which Require Generalization. In *7th International Conference on Learning Representations, ICLR 2019, New Orleans, LA, USA, May 6-9, 2019*. OpenReview.net. <https://openreview.net/forum?id=HkxKH2AcFm>
- [14] Jonathan Ho, Ajay Jain, and Pieter Abbeel. 2020. Denoising Diffusion Probabilistic Models. In *Advances in Neural Information Processing Systems 33: Annual Conference on Neural Information Processing Systems 2020, NeurIPS 2020, December 6-12, 2020, virtual*, Hugo Larochelle, Marc'Aurelio Ranzato, Raia Hadsell, Maria-Florina Balcan, and Hsuan-Tien Lin (Eds.). <https://proceedings.neurips.cc/paper/2020/hash/4c5bfc88584afd967f1ab10179ca4b-Abstract.html>
- [15] Jonathan Ho and Tim Salimans. 2022. Classifier-Free Diffusion Guidance. *CoRR* abs/2207.12598 (2022). <https://doi.org/10.48550/ARXIV.2207.12598> arXiv:2207.12598
- [16] James Jordan, Jinsung Yoon, and Mihaela van der Schaar. 2019. PATE-GAN: Generating Synthetic Data with Differential Privacy Guarantees. In *7th International Conference on Learning Representations, ICLR 2019, New Orleans, LA, USA, May 6-9, 2019*. OpenReview.net. <https://openreview.net/forum?id=S1zk9iRqF7>
- [17] Tero Karras, Samuli Laine, and Timo Aila. 2019. A Style-Based Generator Architecture for Generative Adversarial Networks. In *IEEE Conference on Computer Vision and Pattern Recognition, CVPR 2019, Long Beach, CA, USA, June 16-20, 2019*. Computer Vision Foundation / IEEE, 4401–4410. <https://doi.org/10.1109/CVPR.2019.00453>
- [18] Diederik P. Kingma and Jimmy Ba. 2015. Adam: A Method for Stochastic Optimization. In *3rd International Conference on Learning Representations, ICLR 2015, San Diego, CA, USA, May 7-9, 2015, Conference Track Proceedings*, Yoshua Bengio and Yann LeCun (Eds.). <http://arxiv.org/abs/1412.6980>
- [19] Diederik P. Kingma and Max Welling. 2014. Auto-Encoding Variational Bayes. In *2nd International Conference on Learning Representations, ICLR 2014, Banff, AB, Canada, April 14-16, 2014, Conference Track Proceedings*, Yoshua Bengio and Yann LeCun (Eds.). <http://arxiv.org/abs/1312.6114>
- [20] Junnan Li, Dongxu Li, Caiming Xiong, and Steven C. H. Hoi. 2022. BLIP: Bootstrapping Language-Image Pre-training for Unified Vision-Language Understanding and Generation. In *International Conference on Machine Learning, ICML 2022, 17-23 July 2022, Baltimore, Maryland, USA (Proceedings of Machine Learning Research, Vol. 162)*, Kamalika Chaudhuri, Stefanie Jegelka, Le Song, Csaba Szepesvári, Gang Niu, and Sivan Sabato (Eds.). PMLR, 12888–12900. <https://proceedings.mlr.press/v162/li22n.html>
- [21] Chumeng Liang, Xiaoyu Wu, Yang Hua, Jiaru Zhang, Yiming Xue, Tao Song, Zhengui Xue, Ruhui Ma, and Haibing Guan. 2023. Adversarial Example Does Good: Preventing Painting Imitation from Diffusion Models via Adversarial Examples. In *International Conference on Machine Learning, ICML 2023, 23-29 July 2023, Honolulu, Hawaii, USA (Proceedings of Machine Learning Research, Vol. 202)*, Andreas Krause, Emma Brunskill, Kyunghyun Cho, Barbara Engelhardt, Sivan Sabato, and Jonathan Scarlett (Eds.). PMLR, 20763–20786. <https://proceedings.mlr.press/v202/liang23g.html>
- [22] Luping Liu, Yi Ren, Zhijie Lin, and Zhou Zhao. 2022. Pseudo Numerical Methods for Diffusion Models on Manifolds. In *The Tenth International Conference on Learning Representations, ICLR 2022, Virtual Event, April 25-29, 2022*. OpenReview.net. <https://openreview.net/forum?id=PIKWVd2yBkY>
- [23] Ilya Loshchilov and Frank Hutter. 2019. Decoupled Weight Decay Regularization. In *7th International Conference on Learning Representations, ICLR 2019, New Orleans, LA, USA, May 6-9, 2019*. OpenReview.net. <https://openreview.net/forum?id=Bkg6RiCqY7>
- [24] Shitong Luo and Wei Hu. 2021. Diffusion Probabilistic Models for 3D Point Cloud Generation. In *IEEE Conference on Computer Vision and Pattern Recognition, CVPR 2021, virtual, June 19-25, 2021*. Computer Vision Foundation / IEEE, 2837–2845. <https://doi.org/10.1109/CVPR46437.2021.00286>
- [25] Lingjuan Lyu. 2023. A Pathway Towards Responsible AI Generated Content. In *Proceedings of the Thirty-Second International Joint Conference on Artificial Intelligence, IJCAI 2023, 19th-25th August 2023, Macao, SAR, China*. ijcai.org, 7033–7038. <https://doi.org/10.24963/IJCAI.2023/803>
- [26] Ron Mokady, Amir Hertz, Kfir Aberman, Yael Pritch, and Daniel Cohen-Or. 2023. Null-text Inversion for Editing Real Images using Guided Diffusion Models. In *IEEE/CVF Conference on Computer Vision and Pattern Recognition, CVPR 2023, Vancouver, BC, Canada, June 17-24, 2023*. IEEE, 6038–6047. <https://doi.org/10.1109/CVPR52729.2023.00585>
- [27] Kai Packhäuser, Lukas Folle, Florian Thamm, and Andreas Maier. 2023. Generation of Anonymous Chest Radiographs Using Latent Diffusion Models for Training Thoracic Abnormality Classification Systems. In *20th IEEE International Symposium on Biomedical Imaging, ISBI 2023, Cartagena, Colombia, April 18-21, 2023*. IEEE, 1–5. <https://doi.org/10.1109/ISBI53787.2023.10230346>

- [28] Yiting Qu, Xinyue Shen, Xinlei He, Michael Backes, Savvas Zannettou, and Yang Zhang. 2023. Unsafe Diffusion: On the Generation of Unsafe Images and Hateful Memes From Text-To-Image Models. In *Proceedings of the 2023 ACM SIGSAC Conference on Computer and Communications Security, CCS 2023, Copenhagen, Denmark, November 26-30, 2023*, Weizhi Meng, Christian Damsgaard Jensen, Cas Cremers, and Engin Kirda (Eds.). ACM, 3403–3417. <https://doi.org/10.1145/3576915.3616679>
- [29] Alec Radford, Jong Wook Kim, Chris Hallacy, Aditya Ramesh, Gabriel Goh, Sandhini Agarwal, Girish Sastry, Amanda Askell, Pamela Mishkin, Jack Clark, Gretchen Krueger, and Ilya Sutskever. 2021. Learning Transferable Visual Models From Natural Language Supervision. In *Proceedings of the 38th International Conference on Machine Learning, ICML 2021, 18-24 July 2021, Virtual Event (Proceedings of Machine Learning Research, Vol. 139)*, Marina Meila and Tong Zhang (Eds.). PMLR, 8748–8763. <http://proceedings.mlr.press/v139/radford21a.html>
- [30] Colin Raffel, Noam Shazeer, Adam Roberts, Katherine Lee, Sharan Narang, Michael Matena, Yanqi Zhou, Wei Li, and Peter J. Liu. 2020. Exploring the Limits of Transfer Learning with a Unified Text-to-Text Transformer. *J. Mach. Learn. Res.* 21 (2020), 140:1–140:67. <http://jmlr.org/papers/v21/20-074.html>
- [31] Aditya Ramesh, Prafulla Dhariwal, Alex Nichol, Casey Chu, and Mark Chen. 2022. Hierarchical Text-Conditional Image Generation with CLIP Latents. *CoRR abs/2204.06125* (2022). <https://doi.org/10.48550/ARXIV.2204.06125> arXiv:2204.06125
- [32] Robin Rombach, Andreas Blattmann, Dominik Lorenz, Patrick Esser, and Björn Ommer. 2022. High-Resolution Image Synthesis with Latent Diffusion Models. In *IEEE/CVF Conference on Computer Vision and Pattern Recognition, CVPR 2022, New Orleans, LA, USA, June 18-24, 2022*. IEEE, 10674–10685. <https://doi.org/10.1109/CVPR52688.2022.01042>
- [33] Chitwan Saharia, William Chan, Saurabh Saxena, Lala Li, Jay Whang, Emily L. Denton, Seyed Kamyar Seyed Ghasemipour, Raphael Gontijo Lopes, Burcu Karagol Ayan, Tim Salimans, Jonathan Ho, David J. Fleet, and Mohammad Norouzi. 2022. Photorealistic Text-to-Image Diffusion Models with Deep Language Understanding. In *Advances in Neural Information Processing Systems 35: Annual Conference on Neural Information Processing Systems 2022, NeurIPS 2022, New Orleans, LA, USA, November 28 - December 9, 2022*, Sanmi Koyejo, S. Mohamed, A. Agarwal, Danielle Belgrave, K. Cho, and A. Oh (Eds.). http://papers.nips.cc/paper_files/paper/2022/hash/ec795aeada0b7d230fa35cbaf04c041-Abstract-Conference.html
- [34] Tim Salimans, Ian J. Goodfellow, Wojciech Zaremba, Vicki Cheung, Alec Radford, and Xi Chen. 2016. Improved Techniques for Training GANs. In *Advances in Neural Information Processing Systems 29: Annual Conference on Neural Information Processing Systems 2016, December 5-10, 2016, Barcelona, Spain*, Daniel D. Lee, Masashi Sugiyama, Ulrike von Luxburg, Isabelle Guyon, and Roman Garnett (Eds.). 2226–2234. <https://proceedings.neurips.cc/paper/2016/hash/8a3363abe792db2d8761d6403605aeb7-Abstract.html>
- [35] Pamela Samuelson. 2023. Generative AI meets copyright. *Science* 381, 6654 (2023), 158–161. <https://doi.org/10.1126/science.adi0656> arXiv:https://www.science.org/doi/pdf/10.1126/science.adi0656
- [36] Christoph Schuhmann, Romain Beaumont, Richard Vencu, Cade Gordon, Ross Wightman, Mehdi Cherti, Theo Coombes, Aarush Katta, Clayton Mullis, Mitchell Wortsman, Patrick Schramowski, Srivatsa Kundurthy, Katherine Crowson, Ludwig Schmidt, Robert Kaczmarczyk, and Jenia Jitsev. 2022. LAION-5B: An open large-scale dataset for training next generation image-text models. In *Advances in Neural Information Processing Systems 35: Annual Conference on Neural Information Processing Systems 2022, NeurIPS 2022, New Orleans, LA, USA, November 28 - December 9, 2022*, Sanmi Koyejo, S. Mohamed, A. Agarwal, Danielle Belgrave, K. Cho, and A. Oh (Eds.). http://papers.nips.cc/paper_files/paper/2022/hash/a1859debfb3b59d094f3504d5ebb6c25-Abstract-Datasets_and_Benchmarks.html
- [37] Shawn Shan, Jenna Cryan, Emily Wenger, Haitao Zheng, Rana Hanocka, and Ben Y. Zhao. 2023. Glaze: Protecting Artists from Style Mimicry by Text-to-Image Models. In *32nd USENIX Security Symposium, USENIX Security 2023, Anaheim, CA, USA, August 9-11, 2023*, Joseph A. Calandrino and Carmela Troncoso (Eds.). USENIX Association, 2187–2204. <https://www.usenix.org/conference/usenixsecurity23/presentation/shan>
- [38] Taylor Shin, Yasaman Razeghi, Robert L. Logan IV, Eric Wallace, and Sameer Singh. 2020. AutoPrompt: Eliciting Knowledge from Language Models with Automatically Generated Prompts. In *Proceedings of the 2020 Conference on Empirical Methods in Natural Language Processing, EMNLP 2020, Online, November 16-20, 2020*, Bonnie Webber, Trevor Cohn, Yulan He, and Yang Liu (Eds.). Association for Computational Linguistics, 4222–4235. <https://doi.org/10.18653/V1/2020.EMNLP-MAIN.346>
- [39] Jascha Sohl-Dickstein, Eric A. Weiss, Niru Maheswaranathan, and Surya Ganguli. 2015. Deep Unsupervised Learning using Nonequilibrium Thermodynamics. In *Proceedings of the 32nd International Conference on Machine Learning, ICML 2015, Lille, France, 6-11 July 2015 (JMLR Workshop and Conference Proceedings, Vol. 37)*, Francis R. Bach and David M. Blei (Eds.). JMLR.org, 2256–2265. <http://proceedings.mlr.press/v37/sohl-dickstein15.html>
- [40] Gowthami Somepalli, Vasu Singla, Micah Goldblum, Jonas Geiping, and Tom Goldstein. 2023. Diffusion Art or Digital Forgery? Investigating Data Replication in Diffusion Models. In *IEEE/CVF Conference on Computer Vision and Pattern Recognition, CVPR 2023, Vancouver, BC, Canada, June 17-24, 2023*. IEEE, 6048–6058. <https://doi.org/10.1109/CVPR52729.2023.00586>
- [41] Gowthami Somepalli, Vasu Singla, Micah Goldblum, Jonas Geiping, and Tom Goldstein. 2023. Understanding and Mitigating Copying in Diffusion Models. In *Advances in Neural Information Processing Systems 36: Annual Conference on Neural Information Processing Systems 2023, NeurIPS 2023, New Orleans, LA, USA, December 10 - 16, 2023*, Alice Oh, Tristan Naumann, Amir Globerson, Kate Saenko, Moritz Hardt, and Sergey Levine (Eds.). http://papers.nips.cc/paper_files/paper/2023/hash/9521b6e7f33e039e7d92e23f5e37bbf4-Abstract-Conference.html
- [42] Jiaming Song, Chenlin Meng, and Stefano Ermon. 2021. Denoising Diffusion Implicit Models. In *9th International Conference on Learning Representations, ICLR 2021, Virtual Event, Austria, May 3-7, 2021*. OpenReview.net. <https://openreview.net/forum?id=St1giarCHLP>
- [43] N. Vaidyanathan, C. Raffel, and I. Goodfellow. 2018. Theoretical insights into memorization in GANs. In *Neural Information Processing Systems Workshop*.
- [44] Gerrit J. J. van den Burg and Christopher K. I. Williams. 2021. On Memorization in Probabilistic Deep Generative Models. In *Advances in Neural Information Processing Systems 34: Annual Conference on Neural Information Processing Systems 2021, NeurIPS 2021, December 6-14, 2021, virtual*, Marc’Aurelio Ranzato, Alina Beygelzimer, Yann N. Dauphin, Percy Liang, and Jennifer Wortman Vaughan (Eds.). 27916–27928. <https://proceedings.neurips.cc/paper/2021/hash/eae15aaba768ae4a5993a8a4f4fa6e4-Abstract.html>
- [45] Nikhil Vyas, Sham M. Kakade, and Boaz Barak. 2023. On Provable Copyright Protection for Generative Models. In *International Conference on Machine Learning, ICML 2023, 23-29 July 2023, Honolulu, Hawaii, USA (Proceedings of Machine Learning Research, Vol. 202)*, Andreas Krause, Emma Brunskill, Kyunghyun Cho, Barbara Engelhardt, Sivan Sabato, and Jonathan Scarlett (Eds.). PMLR, 35277–35299. <https://proceedings.mlr.press/v202/vyas23b.html>
- [46] Ryan Webster. 2023. A Reproducible Extraction of Training Images from Diffusion Models. *CoRR abs/2305.08694* (2023). <https://doi.org/10.48550/ARXIV.2305.08694> arXiv:2305.08694
- [47] Yuxin Wen, Neel Jain, John Kirchenbauer, Micah Goldblum, Jonas Geiping, and Tom Goldstein. 2023. Hard Prompts Made Easy: Gradient-Based Discrete Optimization for Prompt Tuning and Discovery. In *Advances in Neural Information Processing Systems 36: Annual Conference on Neural Information Processing Systems 2023, NeurIPS 2023, New Orleans, LA, USA, December 10 - 16, 2023*, Alice Oh, Tristan Naumann, Amir Globerson, Kate Saenko, Moritz Hardt, and Sergey Levine (Eds.). http://papers.nips.cc/paper_files/paper/2023/hash/a00548031e4647b13042c97c922fadf1-Abstract-Conference.html
- [48] Yuxin Wen, Yuchen Liu, Chen Chen, and Lingjuan Lyu. 2024. Detecting, Explaining, and Mitigating Memorization in Diffusion Models. In *The Twelfth International Conference on Learning Representations*. <https://openreview.net/forum?id=84n3UwkH7b>
- [49] Yihan Wu, Hongyang Zhang, and Heng Huang. 2022. RetrievalGuard: Provably Robust 1-Nearest Neighbor Image Retrieval. In *Proceedings of the 39th International Conference on Machine Learning (Proceedings of Machine Learning Research, Vol. 162)*, Kamalika Chaudhuri, Stefanie Jegelka, Le Song, Csaba Szepesvari, Gang Niu, and Sivan Sabato (Eds.). PMLR, 24266–24279. <https://proceedings.mlr.press/v162/wu22o.html>
- [50] Ling Yang, Zhilong Zhang, Yang Song, Shenda Hong, Runsheng Xu, Yue Zhao, Wentao Zhang, Bin Cui, and Ming-Hsuan Yang. 2024. Diffusion Models: A Comprehensive Survey of Methods and Applications. *ACM Comput. Surv.* 56, 4 (2024), 105:1–105:39. <https://doi.org/10.1145/3626235>
- [51] Yuchen Yang, Bo Hui, Haolin Yuan, Neil Gong, and Yinzhi Cao. 2024. Sneakyprompt: Jailbreaking text-to-image generative models. In *2024 IEEE Symposium on Security and Privacy (SP)*. IEEE Computer Society, 123–123.
- [52] Yuxin Zhang, Nisha Huang, Fan Tang, Haibin Huang, Chongyang Ma, Weiming Dong, and Changsheng Xu. 2023. Inversion-based Style Transfer with Diffusion Models. In *IEEE/CVF Conference on Computer Vision and Pattern Recognition, CVPR 2023, Vancouver, BC, Canada, June 17-24, 2023*. IEEE, 10146–10156. <https://doi.org/10.1109/CVPR52729.2023.00978>